Generation of microstripe cylindrical and toroidal mirrors by localized laser evaporation of fused silica

Generation of microstripe cylindrical and toroidal mirrors by localized laser evaporation of fused silica

Krystian L. Wlodarczyk,* Ian J. Thomson, Howard J. Baker, and Denis R. Hall

School of Engineering and Physical Sciences, Heriot-Watt University, Edinburgh EH14 4AS, UK

*Corresponding author: K.L.Wlodarczyk@hw.ac.uk

Received 24 April 2012; revised 9 August 2012; accepted 12 August 2012;
posted 13 August 2012 (Doc. ID 167334); published 7 September 2012

We report a new technique for the rapid fabrication of *microstripe* cylindrical and toroidal mirrors with a high ratio (>10) of the two principal radii of curvature (RoC_1/RoC_2), and demonstrate their effectiveness as mode-selecting resonator mirrors for high-power planar waveguide lasers. In this process, the larger radius of curvature (RoC_1) is determined by the planar or cylindrical shape of the fused silica substrate selected for laser processing, whilst the other (RoC_2) is produced by controlled CO_2 laser-induced vaporization of the glass. The narrow stripe mirror aperture is achieved by applying a set of partially overlapped laser scans, with the incident laser power, the number of laser scans, and their spacing being used to control the curvature produced by laser evaporation. In this work, a 1 mm diameter laser spot is used to produce grooves of cylindrical/toroidal shape with 240 μm width and 16 mm length. After high reflectance coating, these grooves are found to provide excellent mode selectivity as resonator mirrors for a 150 μm core Yb:YAG planar waveguide laser, producing high brightness output at more than 300 W. The results show clearly that the laser-generated *microstripe* mirrors can improve the optical performance of high-power planar waveguide lasers when applied in a low-loss mode-selective resonator configuration.

OCIS codes: 140.3390, 140.3410, 160.6030, 230.7390.

1. Introduction

In this paper, we report the development of an inexpensive CO_2 laser-based technique for the fabrication of *microstripe* cylindrical and toroidal mirrors by the direct writing of controlled-dimension grooves on either planar or curved fused silica substrates, and demonstrate how such structures can be exploited as mode-selective resonator mirrors for high-power planar waveguide lasers. The term *microstripe* is introduced here to describe surfaces with extreme aspect ratio, where the transverse aperture is much less than 1 mm and the transverse sag is in the micrometer range.

The use of the IR wavelength of the CO_2 laser for processing the surface of fused silica by surface melting is now well established. The strong absorption coefficient of the material at the 10.6 μm wavelength gives localized surface heating, whilst the low thermal expansion inhibits crack formation. Flow under surface tension forces creates very smooth surfaces, and early work used the laser polishing effect for increasing the optical damage resistance of silica optics [1], which led to widespread applications in fiber optics [2] and for components in high-energy lasers [3,4]. Recently, more detailed studies have characterized the spatial-frequency response of the CO_2 laser polishing process [5–7], enabling it to be systematically used for finishing micro-optical components [8,9] and more recently macro-optical components [10].

Generally, a surface melt spot diameter of 150–200 μm is appropriate for laser smoothing of

1559-128X/12/266352-09$15.00/0

micromachined fused silica surfaces. The emphasis in these cases is to minimize evaporation of the glass to preserve the surface figure, and this requires close control of the laser conditions and the resultant surface temperature of a workpiece. However, evaporation from the melt pool can be put to use as a surface shaping mechanism when shallow features are required. An example reported recently by three different research groups [11–13] is the fabrication of smooth concave surfaces either on the end facet of a silica fiber or on a silica plate for use as Fabry–Perot microcavity mirrors. In their work, smooth surfaces were produced by a static laser beam focused to the diameter of 40–80 μm at the workpiece, using the regime at which surface evaporation is the dominant process. Depending on the value of the laser power and pulse duration, microcavity mirrors with the sag value in the range of 0.01–4 μm, the aperture between 10 and 60 μm, and the radius of curvature (RoC) in the range of 40–2000 μm were obtained with subnanometer surface roughness.

In this paper, we report on the use of the CO_2 laser evaporation process for the fabrication of *microstripe* mirrors that are suitable as mode-selective resonators for high-power planar waveguide lasers. To achieve this, we use a collimated laser beam with a diameter much larger than that used for the round microcavities described in the previous paragraph, and the workpiece is line-scanned at constant speed under the stationary laser spot. The substrates used in our work are fused silica (Corning HPFS®7980), selected because this material has already been well characterized for CO_2 laser thermal treatment [5–7]. The relatively large beam waist at the workpiece, and consequently the large depth of focus, allows *microstripe* mirrors to be produced on a curved silica substrate without the need for a beam-focus tracking system. This feature enables direct manufacturing of *microstripe* toroidal surfaces with a high ratio of the two principal RoCs ($RoC_1/RoC_2 > 10$).

The main objective of the work covered in this paper is to fabricate biconcave *microstripe* toroidal mirrors that can be used in a low-scattering-loss, mode-selective resonator configuration for a 150 μm core Yb:YAG planar waveguide laser [14] in order to improve the optical performance of this device. To fulfill the resonator requirements, the toroidal mirror must have an aperture of 240 μm in width and 16 mm in length, and the two principal RoCs of 230 and 17 mm. Since such *microstripe* mirrors are not readily available by conventional fabrication techniques, the CO_2 laser-based technique for the manufacture of such optical components has been developed. This method has the advantage of great flexibility of RoC and aperture for the laser resonator applications.

In this paper, *microstripe* grooves produced on the surface of fused silica by single line laser scans, multipass laser scans, and partially overlapping laser scans have been characterized, and the surface quality of these laser-generated structures has been measured and analyzed. The test of selected grooves as laser mirrors within a low-scattering-loss, mode-selective resonator configuration for a 150 μm core Yb:YAG planar waveguide laser has also been reported here.

2. CO_2 Laser Processing Workstation

Figure 1 shows a schematic diagram of the laser processing workstation used for the fabrication of *microstripe* mirrors in fused silica. The system is based on a commercial 300 W average power CO_2 laser (Rofin-Sinar, UK) that is operated with 6 μs RF excitation pulses at a 50 kHz pulse repetition rate. These conditions give a near-CW laser behavior through merging of the effect of excitation pulses. To achieve precise control and stability of the laser power during laser treatment of the glass, the workstation has been equipped with a closed-loop beam power controller based on a thermopile power meter (Gentec, Canada) and an acousto-optic modulator (AOM, NEOS Technologies, USA). The feedback loop used in this system has allowed the laser power fluctuations on the target to be reduced to 1% [measured as the peak-to-valley (P-V) value].

The laser power delivered to the workpiece was provided from the first diffraction order generated by the AOM, with the intensity level of the deflected beam controlled by the AOM voltage. To obtain continuous information on the value of laser power delivered to the target, 33% of the deflected beam was directed to the power meter that sampled the power with a rate of 10 Hz. The 1 mm diameter collimated Gaussian beam on the workpiece front surface was obtained by two appropriate ZnSe lenses. The mechanical shutter situated between the lenses was used to define the length of laser scans. This avoided any upset to the closed-loop beam power controller, which operated continuously. Precise horizontal movement of the workpiece during laser treatment was provided by two stepper motor-driven tables, for both linear and raster scans. The linear scan speed used in all our experiments was 5 mm/s.

Since the absorption coefficient of fused silica varies with wavelength [15] and the CO_2 laser emission spectrum includes possible oscillation lines in the 9–11 μm spectral region, the workstation has been equipped with a spectrum analyzer that provided

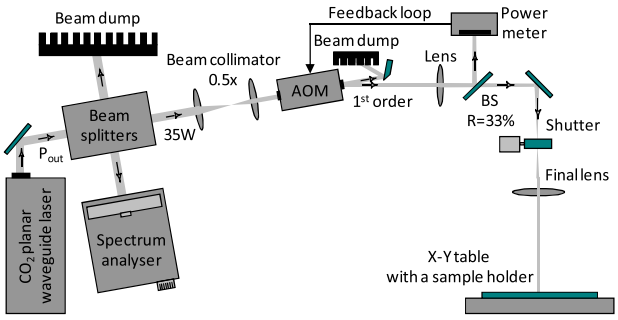

Fig. 1. (Color online) Laser system used for the fabrication of *micro-stripe* mirrors.

continuous monitoring of the laser wavelength. In this work, all substrates were processed with the laser operating only at the single 10.59 μm line. Laser treatment of the glass samples was carried out in air at room temperature. In these experiments, no gas jet was used because the convection plume was sufficient to disperse the small amount of evaporated silica.

3. Characterization of Grooves Produced by Single Line Laser Scans

As shown by our previous research [16], a 1 mm diameter CO_2 laser spot scanning a single line at the speed of 5 mm/s produces permanent, longitudinal grooves on the surface of fused silica (HPFS®7980 Corning) when the laser power delivered to the workpiece exceeds 8.5 W. Grooves produced under such conditions are approximately 200 μm wide and are surrounded by 150 nm deep depressions that can be removed by annealing, as depicted in Fig. 2. As shown by our research [16] and that of Feit *et al.* [17], the depressions are the result of the laser-induced densification of fused silica as a consequence of the local increase of the fictive temperature within the laser-irradiated area. The surface profiles in Fig. 2 have been obtained with a Scantron Proscan 1000 profilometer (UK) fitted with a STILSA chromatic confocal sensor (France). In the experiments described in this paper, the profilometer was set up to take measurements with a 200 μm step in one direction (Y axis) and a 10 μm step in the other (X axis), giving an approximately 20 nm P-V random noise in the height readout.

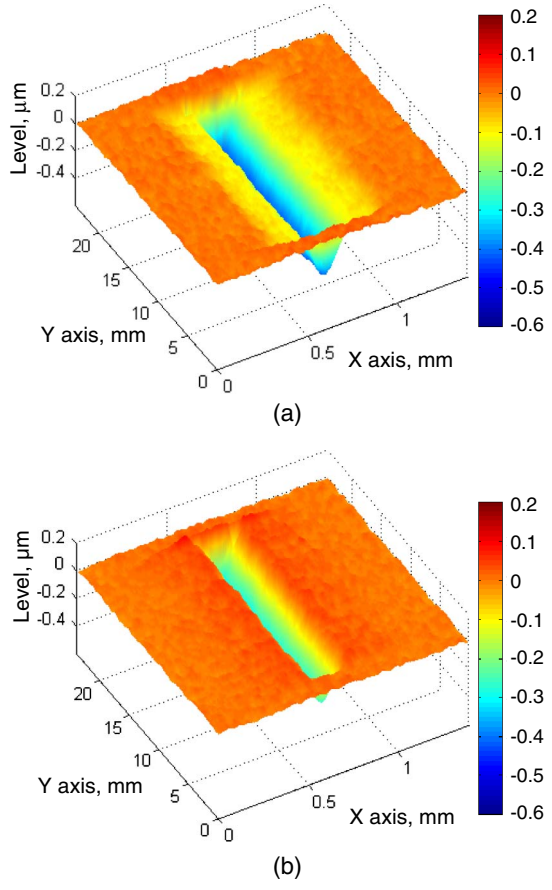

Fig. 2. (Color online) Three-dimensional surface scan of the groove produced by a single line laser scan at $P = 9.4$ W: (a) before and (b) after annealing for 1 h at 1100°C.

Measurements of the average depth of the grooves produced at different values of the laser power for a single linear scan have shown a nonlinear dependency between the groove depth and the laser power used, as can be seen in Fig. 3. These results were obtained for a 1.5 mm thick silica plate that had been annealed for 1 h at a temperature of 1100°C following the laser treatment. The calculated average depth was based on at least 48 depth measurements along a given groove over a 16 mm linear distance.

Inspection of the laser-generated surfaces has revealed that parabolic-shaped grooves are produced up to 9.8 W. Above this power, they become V-shaped and therefore are unsuitable for our laser mirror applications. Using a second-order polynomial fit to the surface profile within the grooves, it has been found that surfaces produced below 9.8 W can be represented quite accurately by a quadratic function of the transverse distance, as shown in Fig. 4. For these grooves, the residue between the fitting function, $f(x)$, and the measured profile, $g(x)$, was determined to be smaller than 50 nm for a distance (ΔW) of 160 μm.

Since the laser-generated grooves were very shallow (<1 μm deep) and relatively wide ($\Delta W \approx 160$ μm), the RoC of these surfaces was calculated based on the coefficients of the fitting function, $f(x)$. Figure 5 shows that the RoC of the grooves decreases in a nonlinear manner with increasing laser power. This relationship results from the fact that a depth of the grooves increases in a nonlinear manner with increasing laser power, as shown in Fig. 3, whereas the width (ΔW) remains almost constant.

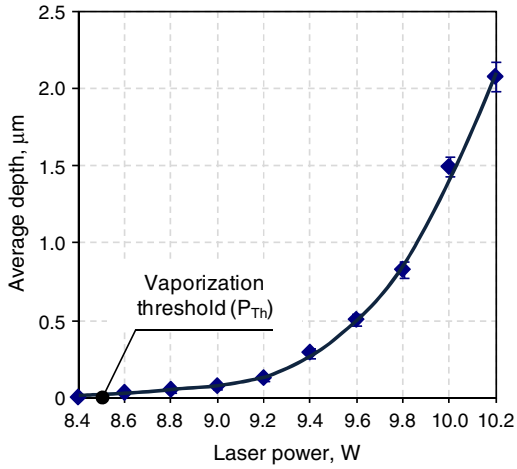

Fig. 3. (Color online) Average depth of the grooves produced at different values of laser power. Results were obtained for a 1.5 mm thick fused silica sample which had been annealed following the laser treatment. Error bars indicate the peak-to-valley magnitude of the surface waviness measured along the bottom of the grooves.

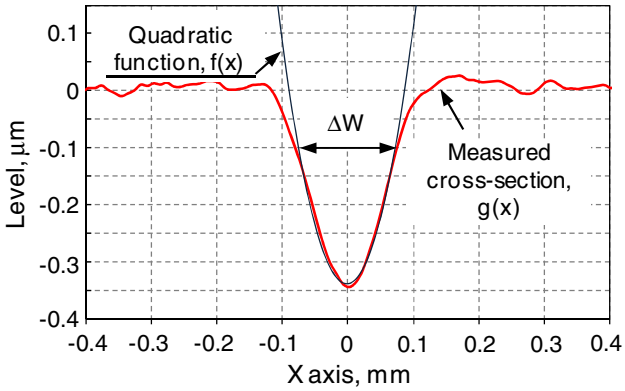

Fig. 4. (Color online) Cross section of the groove produced at $P = 9.5$ W. The surface profile was measured after annealing.

Measurement of the groove depth for different longitudinal positions, as shown in Figs. 6(a) and 6(b), has revealed that the bottom surfaces of the laser-generated grooves suffer from low-spatial-frequency surface irregularities, here referred to as surface waviness. Moreover, as can be concluded from Fig. 6(c), this waviness is more pronounced for the grooves generated at higher values of the laser power. The P-V magnitude of the surface waviness has been found to vary from 60 to 300 nm for the grooves produced in the range of laser powers between 9.2 and 10.2 W. The low surface quality of such grooves, especially those produced at laser powers above 9.6 W, has to be seen as a potential limitation in the fabrication of smooth longitudinal curved surfaces with RoC < 10 mm when the groove is produced by a single line laser scan. Our investigations of the surface imperfections along the groove bottoms has brought us to the conclusion that the waviness results from laser power fluctuations (ΔP) that occur during laser treatment of the glass ($\Delta P \approx 1\%$ P-V of the nominal laser power, as indicated in Section 2) and the fact that the evaporation rate of fused silica increases rapidly with increasing laser power, as shown already in Fig. 3.

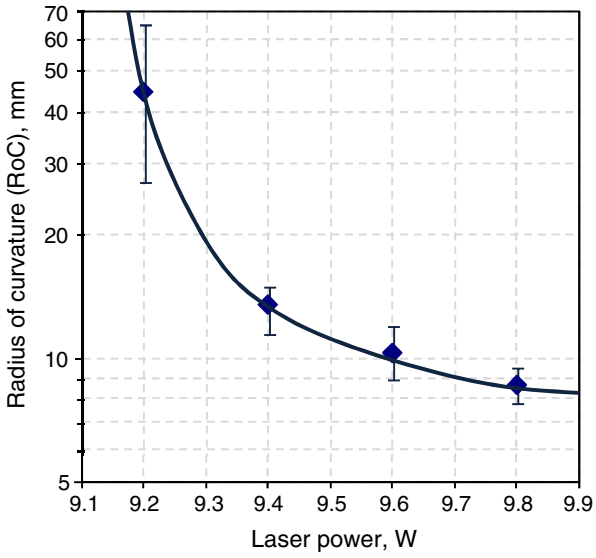

Fig. 5. (Color online) RoC of the grooves produced in the range of laser powers from 9.2 to 9.8 W. Solid line is only a guide for the eye.

4. Characterization of Grooves Produced by Multipass Laser Scans

In this section, we describe the characterization of grooves that were generated by a set of overlapping laser scans. The aim of this work was to determine the relationship between the number of laser scans and the local depth of the laser-generated grooves. As will be shown later, this approach provides a procedure for the fabrication of cylindrical and toroidal mirrors with an aperture that is greater than that generated by a single line laser scan, while avoiding the necessity of increasing the size of the laser beam.

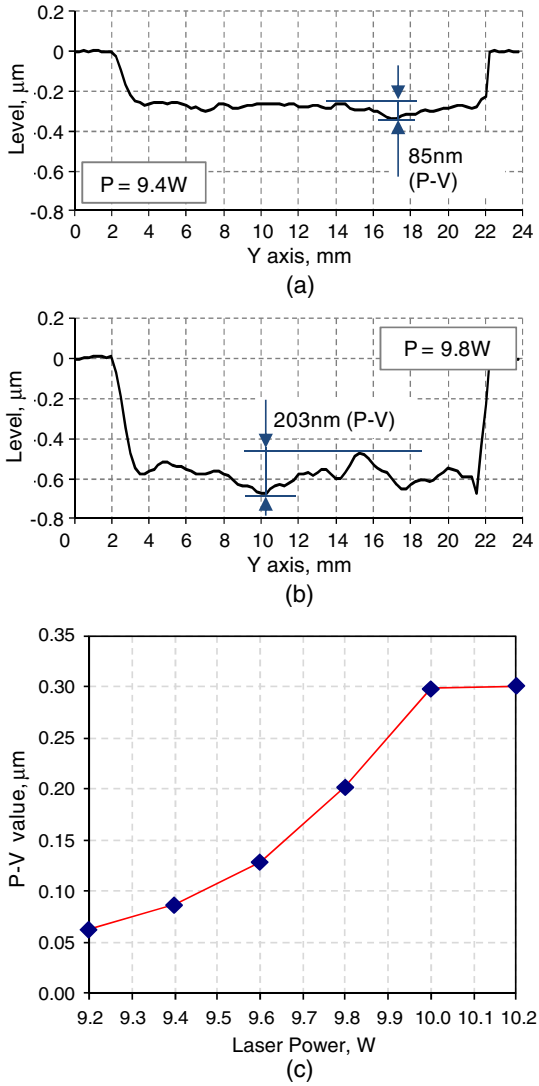

Fig. 6. (Color online) Profile of surface waviness measured along the bottom surface of the laser-generated grooves produced at: (a) $P = 9.4$ W and (b) $P = 9.8$ W. Peak-to-valley (P-V) magnitude of the surface waviness for the grooves produced in the range of laser powers from 9.2 to 10.2 W is shown in (c).

Moreover, we wanted to know how an increasing number of laser scans impacts the surface waviness produced along the bottom of the laser-generated grooves. This knowledge is essential for the fabrication of curved surfaces with minimal surface irregularities required for use as low-scattering-loss laser resonator mirrors.

Figure 7 shows the cross-sections of grooves produced at $P = 9.5$ W by one, two, and five overlapping laser scans, with the other laser machining parameters (i.e., the beam size and the scan speed) set at the same values as those used in the experiments described in Section 3. The surface profiles shown in Fig. 7 have been measured (a) before and (b) after annealing for 1 h at a temperature of 1100°C.

In Fig. 7(a), it can be seen that the grooves become deeper with an increasing number of laser scans (N) due to an accumulative vaporization effect, while the side depressions become slightly shallower. When the glass workpiece is annealed [see Fig. 7(b)], the depressions become bulges because the fictive temperature within the laser-irradiated area is restored to its initial value. We believe that the bulges result from (a) the redeposition of vapor that occurred during laser treatment of the glass and (b) melt movement driven by surface tension forces, also known as the Marangoni effect [18]. As reported by Bennett *et al.* in [18], this effect is more pronounced for longer laser pulses, which in our scanned-CW case is equivalent to increasing the number of laser scans.

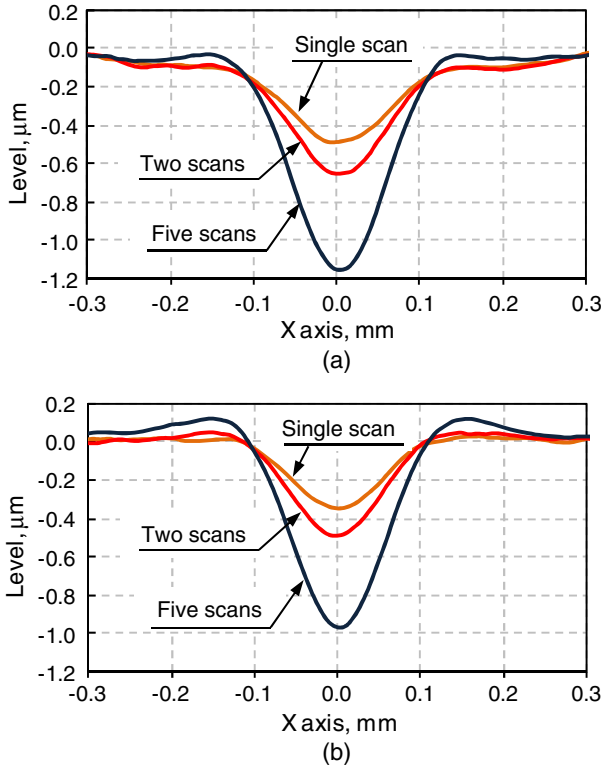

Fig. 7. (Color online) Cross-section of the grooves produced by overlapped laser scans at $P = 9.5$ W. The profiles were measured: (a) before and (b) after annealing for one hour at $T = 1100$ °C.

The average longitudinal depth has been measured for each groove in Fig. 7(b) and plotted in Fig. 8. Although the depth increases in a linear manner with subsequent laser scans, the solid line that joins the measured points for 1, 2, and 5 scans is offset from zero by $D_0 \approx 0.18$ μm. Even though this offset is difficult to explain, it provides strong evidence that fused silica evaporates faster from the "as-manufactured" substrate surface than from the laser-processed surfaces. There are three factors to consider. The *first* is a possible reduction in evaporation rate, associated with a change in surface chemical or compositional state. The *second* is a change in laser coupling, possibly due to an increase of reflectivity at the 10.59 μm wavelength, caused by improved surface smoothness or a shift in complex refractive index from surface composition changes. As an example, the data in Figs. 3 and 8 allow us to estimate the surface reflectivity increase needed to give account for our observations. Based on the experimental data, the reflectivity value would have to increase to approximately 18% relative to its initial value of 15%, as calculated from the complex refractive-index data of Philipp [19]. Finally, laser processing produces a high value of fictive temperature that may affect the thermal conductivity or the surface reflectivity, i.e., the parameters that have significant influence on the laser-induced temperature distribution on the glass surface; see Eq. (3.20) in [20]. Although all above-mentioned suggestions are possible, they require further research because we have not found any related literature on this subject.

The error bars in Fig. 8 are used to indicate P-V magnitude of the surface waviness, which was measured along the bottom of the grooves. The P-V value increases approximately as the square root of the number of laser scans used, thereby indicating that low-frequency laser noise with no correlation between scans is the main effect in causing the waviness. As a consequence, there is a clear advantage to build the groove depth with multipass laser treatment, rather than a single pass with higher laser power.

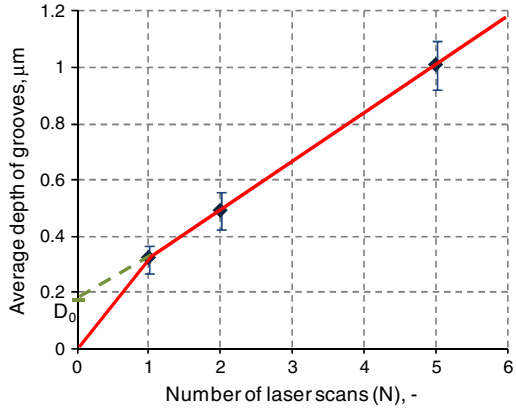

Fig. 8. (Color online) Average depth of grooves shown in Fig. 7(b) as a function of the number of laser scans (N). Error bars indicate the peak-to-valley magnitude of the surface waviness measured along the bottom of the grooves.

5. Fabrication of Grooves by Partial Laser Scan Overlapping

In this section, a technique is presented to control the width and transverse RoC of the laser-generated *microstripe* mirror by using a set of partially overlapped laser scans. As will be shown later, this approach enables the fabrication of the curved surfaces for use as mode-selective mirrors in a low-coupling-loss resonator configuration for a 150 μm core Yb:YAG planar waveguide laser [14]. According to Degnan and Hall [21], mode-selectivity is obtained when a mirror with a transverse RoC two times the free-space Rayleigh range for the lowest-order waveguide mode is placed at the Rayleigh distance from the waveguide end-facet. For the Yb:YAG laser, this is achieved when the resonator mirror has the RoC of 17.2 mm and its transverse aperture is at least 220 μm full width.

Moreover, this section demonstrates how the *microstripe* surfaces can be written on a curved substrate in order to produce mode-selective toroidal mirrors for improving the optical performance of the planar waveguide lasers in *both* transverse and lateral directions. To demonstrate this with the Yb:YAG laser, we aim to fabricate a *microstripe* toroidal mirror with the two principal RoCs close to 17 and 230 mm.

A. Subtractive Model

As shown in Section 4, the depth of the grooves increases in a linear manner with increasing number of the subsequent laser scans. Therefore, it is possible to use a simple subtractive model to predict the final shape of the grooves produced by partial laser scan overlapping. The model is based on the assumption that the resultant surface profile, $G(x)$, is the sum of N constituent surface profiles, $g(x)$.

Figure 9 shows an example of the use of the subtractive model. Here, $g(x)$ represents a Gaussian function that best fits the cross section of the groove produced by a single line laser scan at a laser power of 9.5 W, whereas $G(x)$ represents the profile that is the sum of five Gaussian functions, $g(x)$, shifted with respect to each other by a distance of $\Delta x = 46$ μm. For these conditions, the RoC of the function $G(x)$ in the range between −120 and 120 μm has been determined to be approximately 16 mm, and thus matches closely the mirror requirements for the Yb:YAG planar waveguide laser.

In order to demonstrate the validity of the subtractive model, we performed an experiment in which a 1.5 mm thick plate of fused silica was treated by five partially overlapping laser scans at $P = 9.5$ W and with a spacing $\Delta x = 46$ μm. As can be seen in Fig. 9, the groove produced under these machining conditions is similar in shape to the profile that was determined with the aid of the subtractive model. Taking account of the offset $D_0 \approx 180$ nm, which resulted from the first laser scan (see Fig. 8), the difference between the experimental results and the theoretical predictions has been evaluated to be as small as

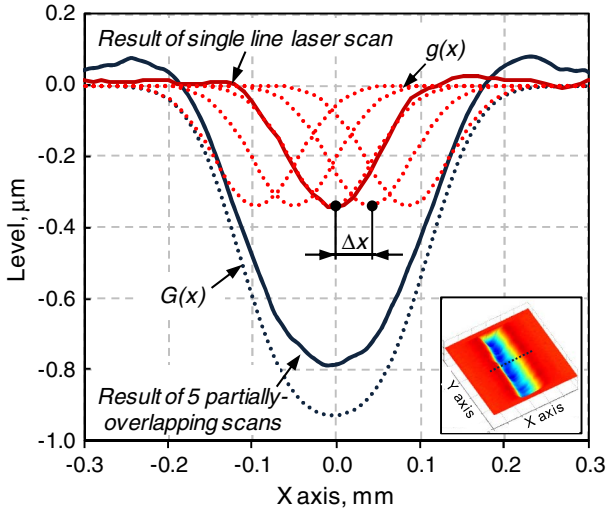

Fig. 9. (Color online) Cross-section of the groove produced by five partially overlapping laser scans at $P = 9.5$ W and with a 46 μm spacing (Δx) between individual laser scans. Dotted curves represent the profiles determined with the aid of the subtractive model, whereas the solid curves represent the experimental results.

0.1 μm P-V. Therefore, it can be concluded that the aperture of the grooves can be successfully increased by using a set of partially overlapped laser scans and the RoC of these grooves can be predicted with the aid of the subtractive model.

B. Fabrication of Toroidal Mirrors

In this subsection, a commercially available uncoated cylindrical lens made of fused silica is treated by a set of partially overlapped laser scans. The thickness of this lens varies from 3 mm at the center line to 3.5 mm at the edges. By measuring the surface profile of the lens along its curvature and applying the second-order polynomial fitting approach, as described in Section 3, the RoC of the lens was determined to be 226 mm. This value matches closely the target RoC value of 230 mm that is required for a mode-selective resonator setup for a 150 μm core Yb:YAG planar waveguide laser.

To generate the desired curvature along the transverse direction, partially overlapping laser scans were carried out along the lens curvature, thereby producing a toroidal shape. The scan speed, the number of laser scans, and the spacing between them were the same as those used to produce the 16 mm RoC cylindrical groove described in Subsection 5.A. The laser power was reduced slightly because the laser-generated grooves tend to be deeper when a thicker substrate is applied [16]. Since the cross section of the grooves produced by a single line laser scan was unknown for a 3 mm thick sample, four mirror sections were fabricated on one cylindrical surface. In this approach, each mirror was generated using a slightly different value of the laser power between 9.30 and 9.45 W.

The RoC values of the laser-machined toroidal surfaces are listed in Table 1. The radii were measured after annealing of the glass substrate, using the

Table 1. Laser Power and Laser Power Fluctuations (ΔP) Measured during Laser Scanning, the RoC of the Grooves in the X and Y Axis, and the Peak-to-Valley Magnitude of the Surface Waviness Measured along the Bottom of each Groove

Groove No.	Power, W	ΔP, mW	RoC_X, mm	RoC_Y, mm	P-V Value, μm
1	9.30	−30/ + 20	21.3	226	0.17
2	9.35	−22/ + 29	20.1	226	0.23
3	9.40	−36/ + 25	12.9	226	0.38
4	9.45	−27/ + 24	12.3	226	0.25

same annealing procedure as that described in the previous sections. Table 1 also contains the laser power fluctuations (ΔP), which were recorded by the power meter during laser scanning, and the P-V magnitude of the surface waviness, which was measured along the bottom of the grooves within a 16 mm distance. The waviness was measured relative to the untreated surface level, so that the effects of any surface irregularities that had initially been in the substrate were cancelled out.

The laser-generated surface, which is the closest match to the geometrical requirements for the toroidal mirror specified at the beginning of Section 5, has been fabricated at an average laser power of 9.35 W. The overall shape of this surface is shown in Fig. 10(a), whilst the surface waviness measured along its bottom is presented in Fig. 10(b).

Finally, it should be noted that the variation of the width of the laser-generated mirror was negligible along the Y axis. This indicates that with a 1 mm diameter beam waist delivered to the target there is no problem with focus change over the approximately 0.5 mm depth (sag) of the lens used as the substrate. Thus, the process described in this paper has a significant advantage over a conventional laser micromachining approach, allowing processing of toroidal surfaces without any expensive beam-focus tracking system, thus reducing the overall cost of the fabrication process.

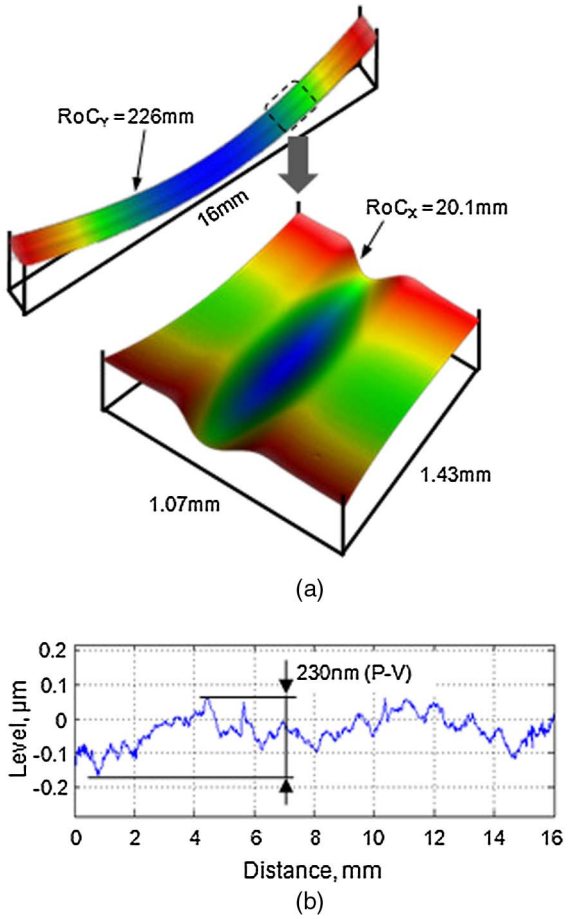

Fig. 10. (Color online) (a) Overall shape and close-up view of the *microstripe* toroidal mirror produced by five laser scans with $\Delta x = 46$ μm and at $P = 9.35$ W. Surface waviness measured along the bottom of the mirror is shown in (b).

6. Test of the Laser-Generated Grooves as Laser Resonator Mirrors

The 16 mm RoC cylindrical groove described in Subsection 5.A and the toroidal surfaces from Subsection 5.B have been tested as the rear mirrors in a mode-selective resonator configuration designed for a 150 μm core Yb:YAG planar waveguide laser. In previous operation with conventional non-mode-selective mirrors [14], the Yb:YAG laser generated a multimode output power of approximately 400 W with a maximum incident pump power of 800 W.

A. Cylindrical Groove

Figure 11 shows the optical arrangement of the resonator used for testing the 16 mm RoC *microstripe* cylindrical surface, after dielectric coating giving 90% reflectivity for the 1030 nm laser wavelength. The configuration is designed to be waveguide mode-selective in the transverse (X) direction and multimode stable in the lateral (Y) direction. The 80% reflectivity plane output mirror was placed very close (0.5 mm) to the waveguide end-facet. The laser-fabricated *microstripe* cylindrical mirror under test was aligned at a plane 8 mm from the opposite

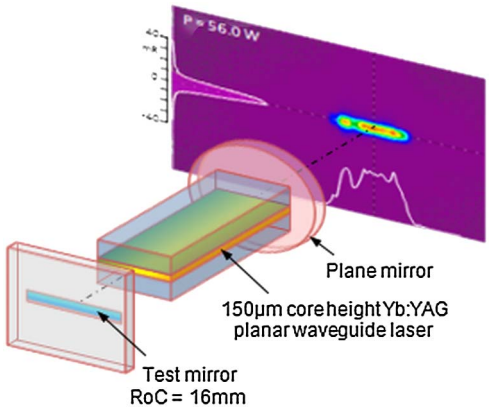

Fig. 11. (Color online) Laser beam profile obtained from the Yb:YAG planar waveguide laser when the 16 mm RoC cylindrical groove was applied as a mirror in the low-loss mode-selective resonator configuration.

waveguide end-facet. Since the 8 mm distance almost corresponded to the Rayleigh range of the lowest-order waveguide mode and was one-half the magnitude of the RoC of the test structure, the *microstripe* mirror offered mode selectivity by coupling efficiently only the fundamental waveguide mode into the laser core. This type of waveguide mode-selection design arrangement is described in detail in [21]. To capture the laser beam profile, a diffusive screen was placed a distance of 250 mm from the plane mirror and the image was recorded by a CCD camera.

The cylindrical *microstripe* mirror was relatively easy to align because there was a large change in both output power and beam profile when the mirror was moved away from optimum vertical alignment. The output laser beam profile in the vertical direction for the aligned test mirror, which is shown in Fig. 11, has been found to match closely the theoretical TE_1 waveguide mode propagating in air. Even though some extra power in the side lobes has been observed, due to either weak higher-order modes or diffraction coming from the edges of the groove structure, this result shows successful operation of the cylindrical groove as the mode-selective mirror for planar waveguide lasers.

As expected, in the lateral direction, the laser behaves as a highly multimode stable resonator. Therefore, in this experiment it was not possible to assess the impact of the residual surface waviness along the groove bottom (*microstripe* mirror axis) on the output laser beam quality.

Finally, this proof-of-principle initial test of the laser-generated cylindrical mirror was performed only at a relatively low pump/output power because the coating applied to the *microstripe* mirror had an unknown value of laser damage threshold and a 10% leakage. Since possible damage of the coating could result in catastrophic damage to the (expensive) planar waveguide, due to the mirrors being situated very close to the waveguide end-facets, the test was only performed at values of incident pump power below 250 W, thereby yielding a maximum output power of only 56 W.

B. Toroidal Surfaces

The laser-generated *microstripe* toroidal surfaces have been tested in the same optical arrangement as that shown in Fig. 11. In order to explore the toroidal surfaces for the maximum incident pump power of 800 W, the substrate with grooves was coated with a laser-grade HR layer that could work safely with high intensities at 1030 nm. In general, the *microstripe* toroidal mirrors were able to cope with an output power of 326 W, giving at the same time an excellent output beam profile in the transverse direction. This result allows us to state that the laser-generated *microstripe* cylindrical and toroidal mirrors can easily work with high-power planar waveguide lasers. Moreover, by using a laser-generated *microstripe* toroidal mirror with RoC values that match closely the conditions for a negative branch unstable resonator, the output beam quality of the planar waveguide lasers can be successfully improved in *both* transverse and lateral directions. Preliminary results of this experiment have been presented recently at the OSA Advanced Solid-State Photonics meeting [22].

7. Conclusions

This paper has reported a novel approach for rapid prototyping (fabrication) of fused silica *microstripe* toroidal mirrors with a high ratio of the two principal RoCs ($RoC_1/RoC_2 > 10$). In this process, one RoC (RoC_1) is determined by the shape of the substrate used for machining, whilst the other RoC (RoC_2) is achieved by CO_2 laser-induced vaporization of the glass. Generally, the curvature produced by evaporation can be controlled by the size of the laser spot, the laser power, the number of laser scans, and the spacing between them.

A notable feature of the laser-generated *microstripe* mirrors is their relative (X-Y) dimensions. Since the mirrors have been produced by a low number of partially overlapped laser scans, they combine *both* adequate length in the lateral direction, to match the size of the planar waveguides, and very narrow dimensions, which are required for transverse waveguide mode selectivity. The mirror width is in the region of a few hundred micrometers due to the fact that they were produced by an approximately 1 mm diameter laser beam. Nevertheless, *microstripe* toroidal mirrors with a smaller aperture may also be fabricated using this process but with reduced beam diameter. Thus, this type of optical components can be used with the planar waveguide lasers that are characterized by a core size smaller than 150 μm.

The successful operation of the laser-generated *microstripe* cylindrical and toroidal mirrors in mode-selective resonator configurations for high-power planar waveguide lasers has been described in this paper, showing that this kind of optical component can perform very well at the laser output power levels of at least 300 W. Our preliminary experiment with the toroidal mirror used as a mode selector in a negative branch low-loss unstable resonator configuration with a 150 μm core Yb:YAG planar waveguide laser has shown that the laser beam profile can be improved in *both* transverse and lateral directions. To the authors' knowledge, this is the first time that this kind of component has been fabricated and demonstrated in use with a high-power planar waveguide laser resonator.

Future work is directed at producing further reduction of the surface waviness along the bottom of the laser-generated *microstripe* mirrors, whereupon the CO_2 laser-based technique described in this paper may be able to compete with diamond turning, which is typically used for the fabrication of conventional, large aperture toroidal mirrors.

The research covered in this paper was funded by the Engineering and Physical Sciences Research

Council (EPSRC) as part of the Innovative Manufacturing Research Centre (IMRC) at Heriot-Watt University. In addition, partial financial support for this project from PowerPhotonic Ltd is acknowledged.

References

1. P. A. Temple, W. H. Lowdermilk, and D. Milam, "Carbon dioxide laser polishing of fused silica surfaces for increased laser-damage resistance at 1064 nm," Appl. Opt. **21**, 3249–3255 (1982).
2. A. Kuhn, P. French, D. P. Hand, I. J. Blewett, M. Richmond, and J. D. C. Jones, "Preparation of fiber optics for the delivery of high-energy high-beam-quality Nd: YAG laser pulses," Appl. Opt. **39**, 6136–6143 (2000).
3. R. M. Brusasco, B. M. Penetrante, J. A. Butler, S. M. Maricle, and J. E. Peterson, "CO_2-laser polishing for reduction of 351 nm surface damage initiation in fused silica," Proc. SPIE **4679**, 34–39 (2001).
4. R. R. Prasad, J. R. Bruere, J. Peterson, J. M. Halpin, M. Borden, and R. P. Hackel, "Enhanced performance of large 3ω optics using UV and IR lasers," Proc. SPIE **5273**, 288–295 (2004).
5. K. M. Nowak, H. J. Baker, and D. R. Hall, "Efficient laser polishing of silica micro-optic components," Appl. Opt. **45**, 162–171 (2006).
6. E. Mendez, K. M. Nowak, H. J. Baker, F. J. Villarreal, and D. R. Hall, "Localized CO_2 laser damage repair of fused silica optics," Appl. Opt. **45**, 5358–5367 (2006).
7. K. L. Wlodarczyk, E. Mendez, H. J. Baker, R. McBride, and D. R. Hall, "Laser smoothing of binary gratings and multilevel etched structures in fused silica," Appl. Opt. **49**, 1997–2005 (2010).
8. J. F. Monjardin, K. M. Nowak, H. J. Baker, and D. R. Hall, "Correction of beam errors in high power laser diode bars and stacks," Opt. Express **14**, 8178–8183 (2006).
9. N. Trela, H. J. Baker, J. J. Wendland, and D. R. Hall, "Dual-axis beam correction for an array of single-mode diode laser emitters using a laser-written custom phase-plate," Opt. Express **17**, 23576–23581 (2009).
10. S. Heidrich, E. Willenborg, and A. Richmann, "Development of a laser based process chain for manufacturing freeform optics," Phys. Procedia **12**, 519–528 (2011).
11. R. J. Barbour, P. A. Dalgarno, A. Curran, K. M. Nowak, H. J. Baker, D. R. Hall, N. G. Stoltz, P. M. Petroff, and R. J. Warburton, "A tunable microcavity," J. Appl. Phys. **110**, 053107 (2011).
12. D. Hunger, T. Steinmetz, Y. Colombe, C. Deutsch, T. W. Hänsch, and J. Reichel, "A fiber Fabry–Perot cavity with high finesse," New J. Phys. **12**, 065038 (2010).
13. C. Toninelli, Y. Delley, T. Stöferle, A. Renn, S. Götzinger, and V. Sandoghdar, "A scanning microcavity for in situ control of single-molecule emission," Appl. Phys. Lett. **97**, 021107 (2010).
14. I. J. Thomson, J. F. Monjardin, H. J. Baker, and D. R. Hall, "Efficient operation of a 400 W diode side-pumped Yb:YAG planar waveguide laser," IEEE J. Quantum Electron. **47**, 1336–1345 (2011).
15. A. D. McLachlan and F. P. Meyer, "Temperature dependence of the extinction coefficient of fused silica for CO_2 laser wavelengths," Appl. Opt. **26**, 1728–1731 (1987).
16. K. L. Wlodarczyk, "Surface deformation mechanisms in laser smoothing and micro-machining of optical glasses," Ph.D. dissertation (Heriot-Watt University, 2011).
17. M. D. Feit, M. J. Matthews, T. F. Soules, J. S. Stolken, R. M. Vignes, S. T. Yang, and J. D. Cooke, "Densification and residual stress induced by CO_2 laser-based mitigation of SiO_2 surfaces," Proc. SPIE **7842**, 78420O (2010).
18. T. D. Bennett, D. J. Krajnovich, C. P. Grigoropoulos, P. Baumgart, and A. C. Tam, "Marangoni mechanism in pulsed laser texturing of magnetic disk substrates," J. Heat Transfer **119**, 589–596 (1997).
19. H. R. Philipp, "Silicon dioxide (SiO_2) glass," in *Handbook of Optical Constants of Solids*, E. D. Palik, ed. (Academic, 1985), pp. 749–763.
20. M. Von Allmen and A. Blatter, *Laser-Beam Interactions with Materials: Physical Principles and Applications* (Springer Verlag, 1995).
21. J. J. Degnan and D. R. Hall, "Finite-aperture waveguide laser resonators," IEEE J. Quantum Electron. **9**, 901–910 (1973).
22. I. J. Thomson, K. L. Wlodarczyk, D. R. Hall, and H. J. Baker, "High brightness Yb:YAG planar waveguide laser with an unstable resonator formed with a novel laser-machined, toroidal mode-selective mirror," in *Advanced Solid-State Photonics*, OSA Technical Digest (CD), (Optical Society of America, 2012), paper AW4A.19.